Mass spectrometry captures off-target drug binding and provides mechanistic insights into the human metalloprotease ZMPSTE24

Shahid Mehmood[1], Julien Marcoux[1], Joseph Gault[1], Andrew Quigley[2], Susan Michaelis[3], Stephen G. Young[4], Elisabeth P. Carpenter[2], and Carol V. Robinson[1]*

[1]Department of Chemistry, University of Oxford, South Parks Road, Oxford OX1 3QZ UK

[2]Structural Genomics Consortium, University of Oxford, Old Road Campus Research Building, Roosevelt Drive, Oxford, OX3 7DQ, UK

[3]Department of Cell Biology, The Johns Hopkins School of Medicine, Baltimore, MD 21205, USA

[4]Departments of Medicine and Human Genetics, David Geffen School of Medicine; University of California, Los Angeles, CA 90095 USA

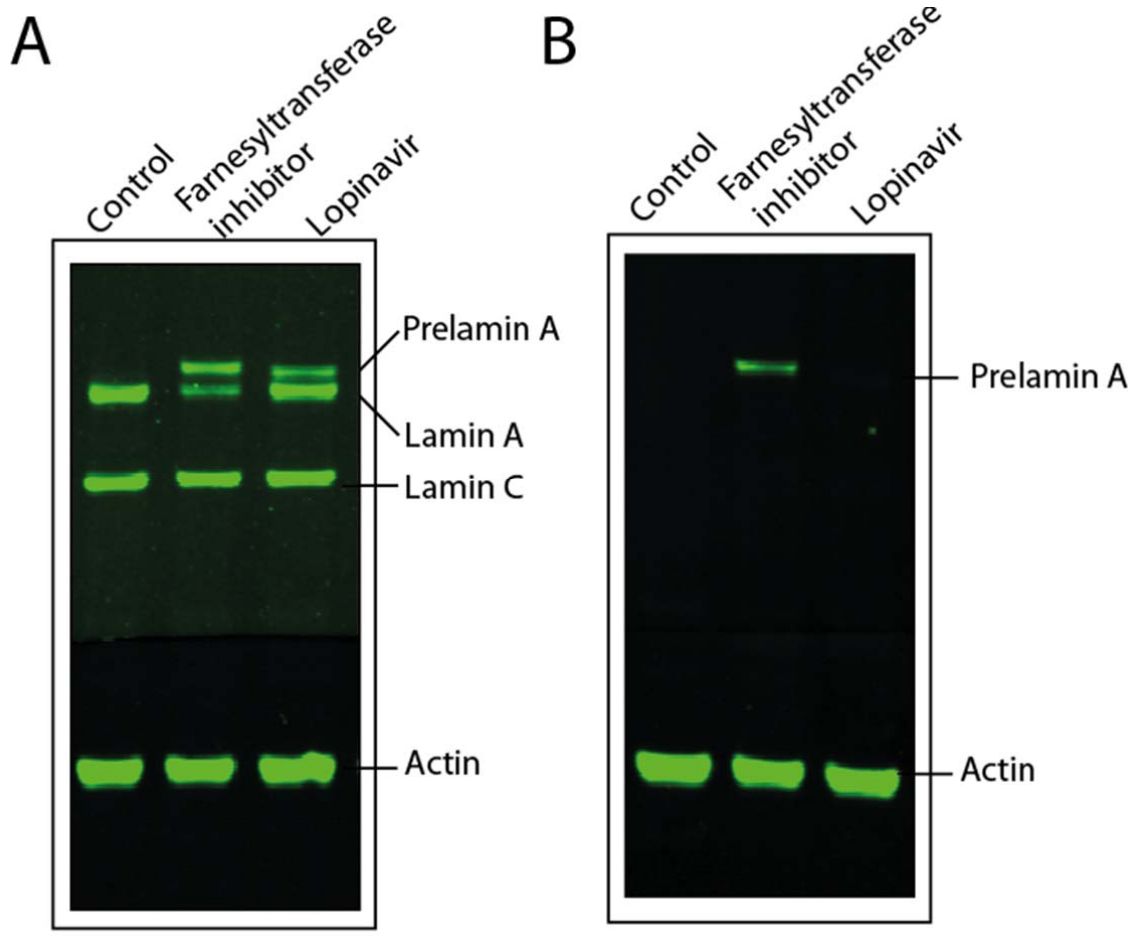

Figure S1. Western blots of cell extracts from a human fibroblast cell line that was exposed to a protein farnesyltransferase inhibitor (ABT-100, 0.5 μM) or lopinavir (20 μM) for three days. The cell extracts were size-fractionated on 4–12% polyacrylamide-SDS gels and proteins were transferred to nitrocellulose membranes for western blotting. Membranes were cut in half; the bottom half was incubated with a goat IgG against actin (as a loading control); the top half was incubated with either a goat IgG against human lamin A/C (panel A) or a rat monoclonal antibody against prelamin A (panel B) (monoclonal antibody 7G11; created by immunizing a rat with a synthetic peptide corresponding to the last 15 amino acids of mouse prelamin A)[1]. In the case of *mouse* prelamin A, monoclonal antibody 7G11 detects both farnesylated and nonfarnesylated prelamin A. However, for *human* prelamin A, the antibody is *specific* for nonfarnesylated prelamin A. Binding of the primary antibodies was detected by incubating the membranes with an IRDye-conjugated donkey anti–goat IgG or an IRDye-conjugated donkey anti–rat IgG; bands were visualized with the Odyssey Infrared Imaging System (Li-Cor Biosciences). An accumulation of prelamin A is clearly observed in the presence of both the protein farnesyltransferase inhibitor and lopinavir. Note that the *nonfarnesylated* prelamin A in the protein farnesyltransferase–treated fibroblasts has a slower electrophoretic mobility than the farnesyl–prelamin A in lopinavir-treated cells.

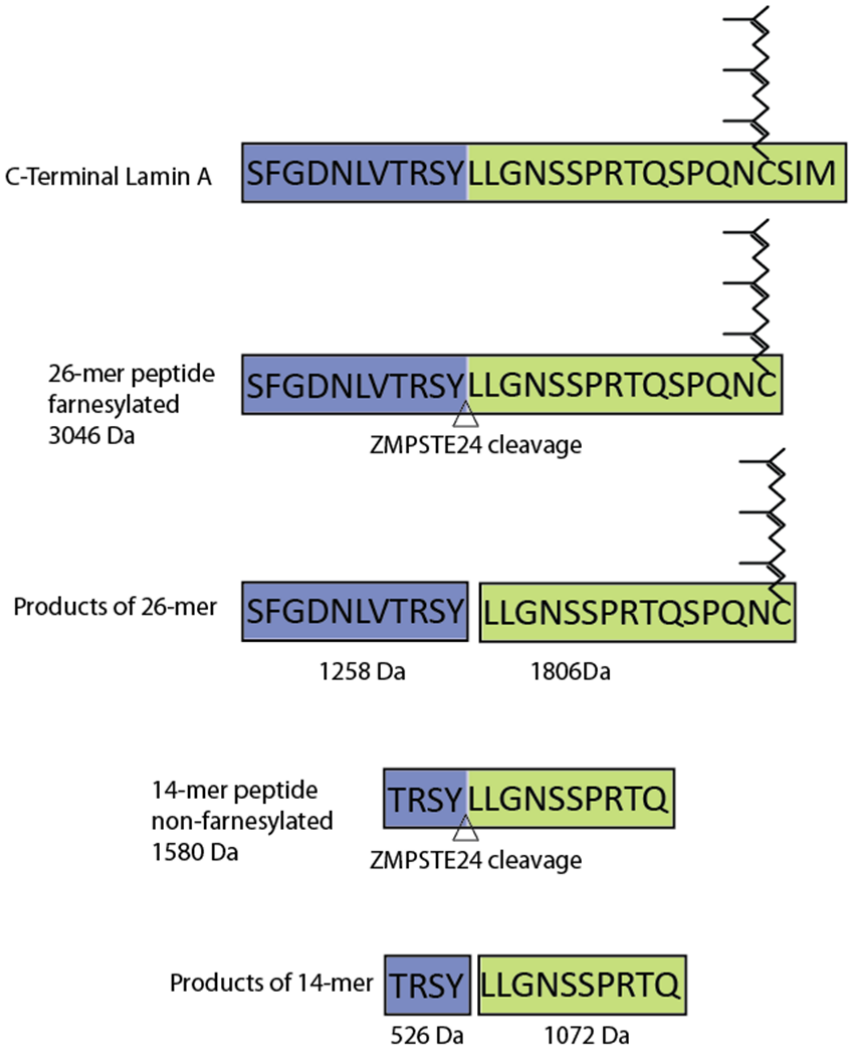

Figure S2. Amino acid sequences and molecular weights of substrate petide and their respective products.

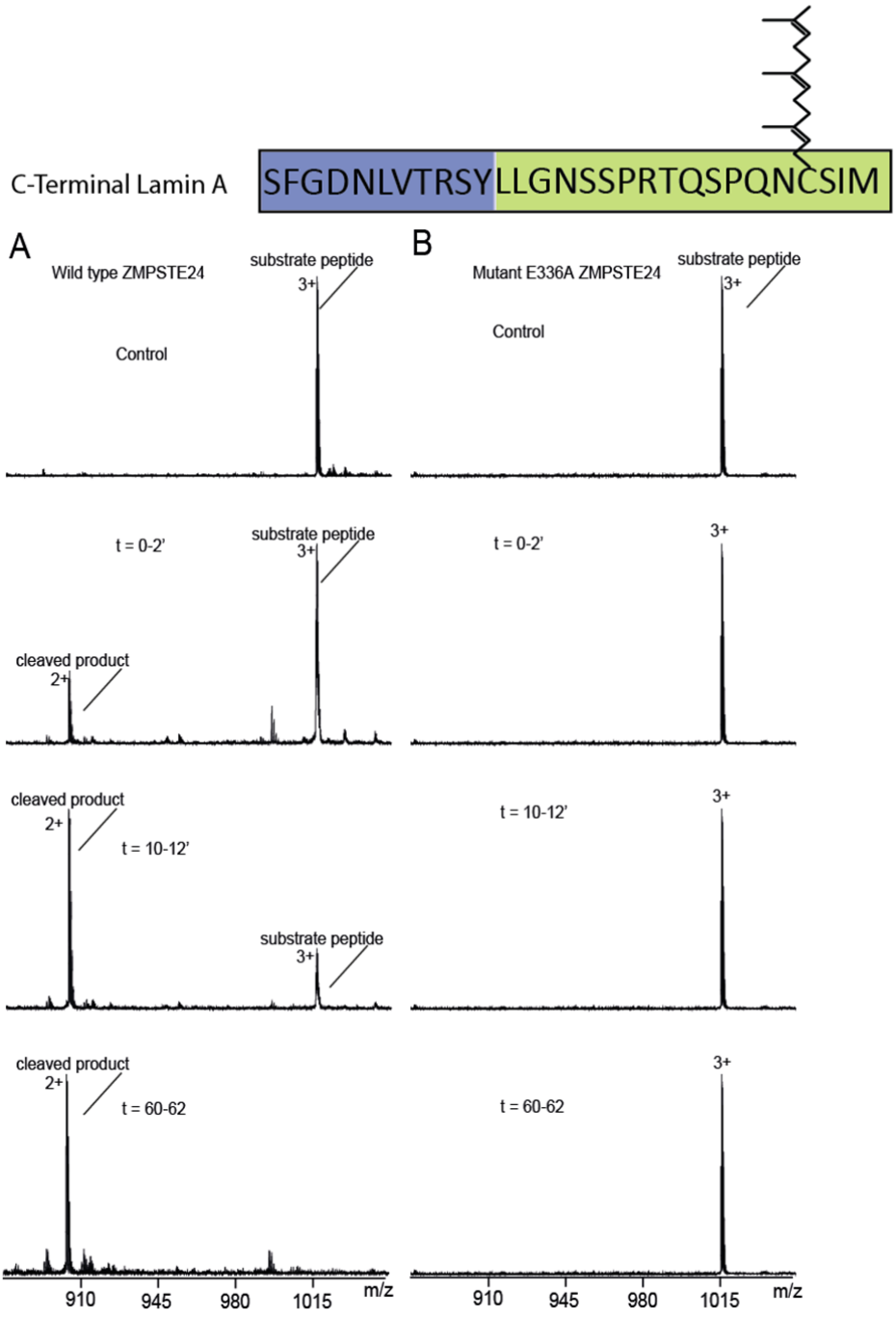

Figure S3 . Mass spectra of the farnesylated substrate peptide after inubation with the wild-type (a) and the mutant E336A ZMPSTE24 (b). When incubated with the wild-type protein, a decrease in the intensity of the substrate peptide and an increased instensity of cleaved product is evident with time. In the case of mutant ZMPSTE24, the substrate peptide remains undigested. Upper panel shows the control (*i.e.*, substrate peptide without any ZMPSTE24).

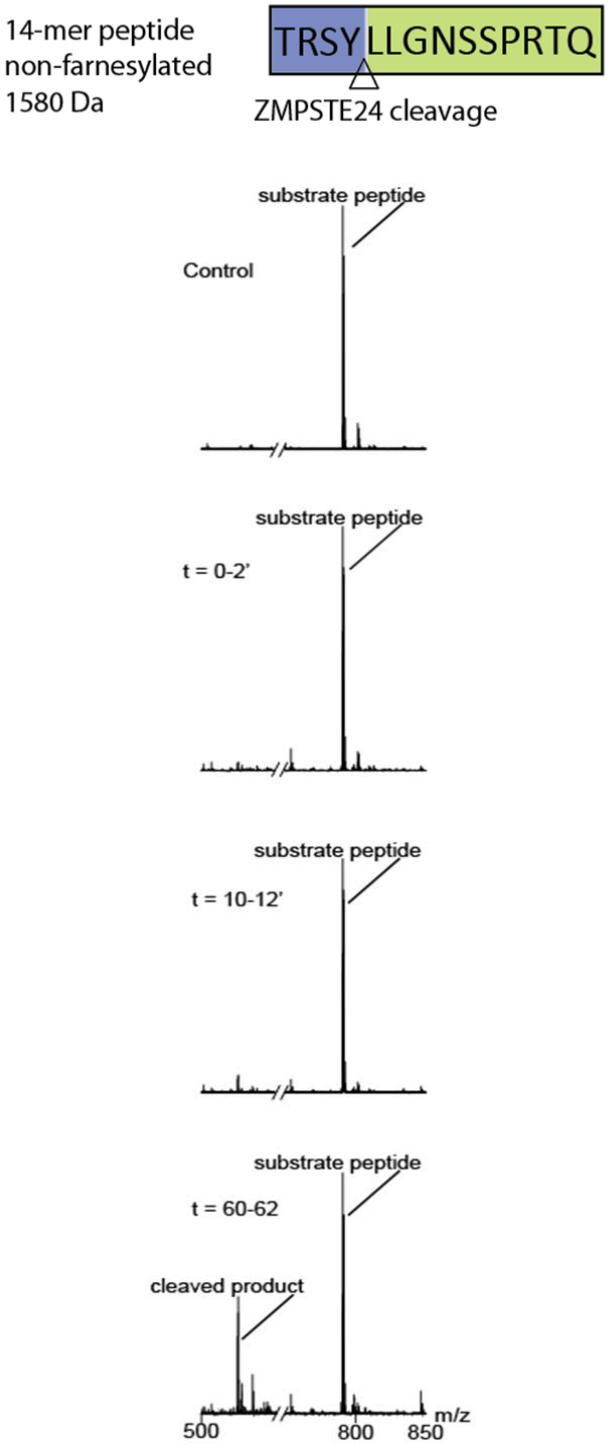

Figure S4. Mass spectra of the nonfarnesylated 14-mer peptide. The substrate remains essentially uncleaved after 10-12' and only modestly cleaved after a 1-h incubation.

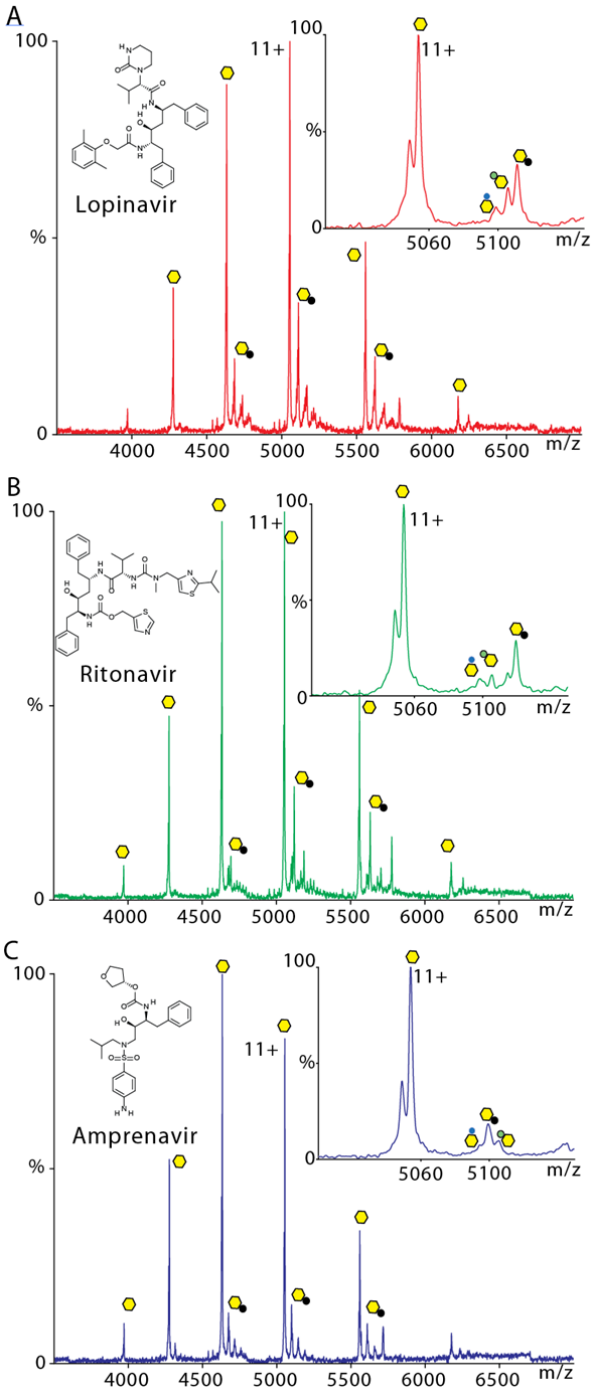

Figure S5**.** Binding of HIV protease inhibitor drugs to ZMPSTE24. High resolution Orbitrap mass spectra show the interaction between ZMPSTE24 and lopinavir, ritonavir, and amprenavir. The mass spectrometry conditions and concentrations of protein and drugs was kept constant. Charge state series are labelled: yellow hexagon, zinc-bound ZMPSTE24; green circle, ZMPSTE24·CHS; blue circle, ZMPSTE24·OGNG; black circle, binding of respective drugs. Insets show chemical structures and expansion of the 11+ charge state.

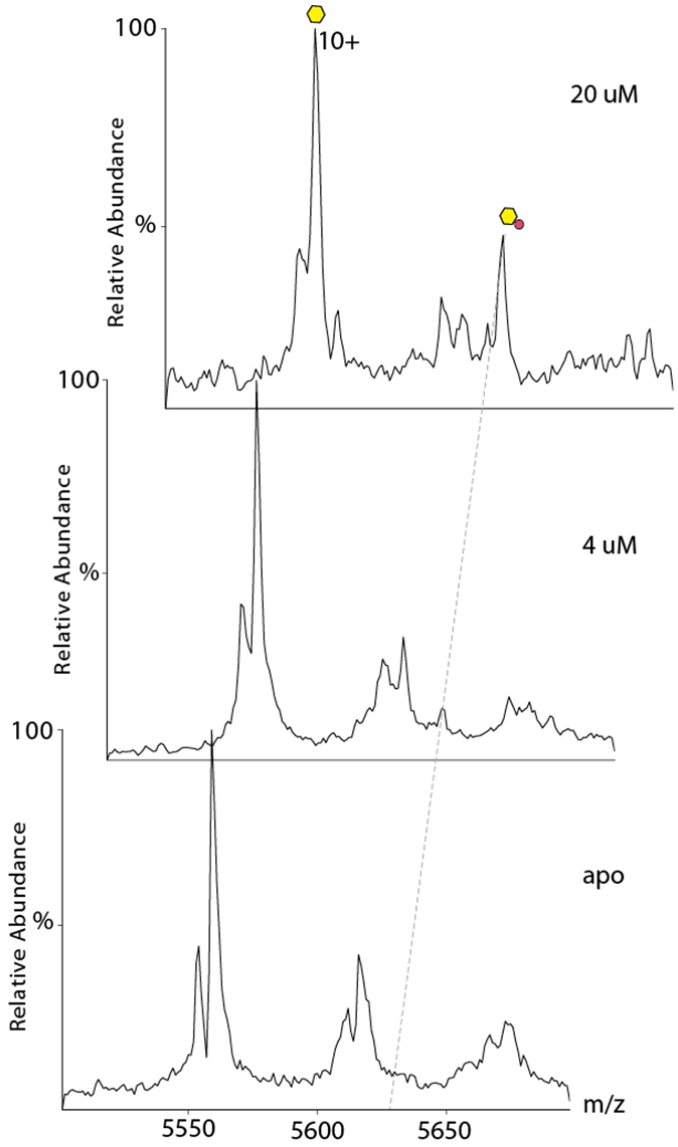

Figure S6. Concentration dependence of ritonavir binding to ZMPSTE24. Mass spectra of 10+ charge state of ZMPSTE24 (lower panel) in the presence of 4 uM and 20 uM ritonavir (upper panels). An increase in the peak intensity assigned to the ZMPSTE24–ritonavir conjugate is clearly shown with a dashed line.

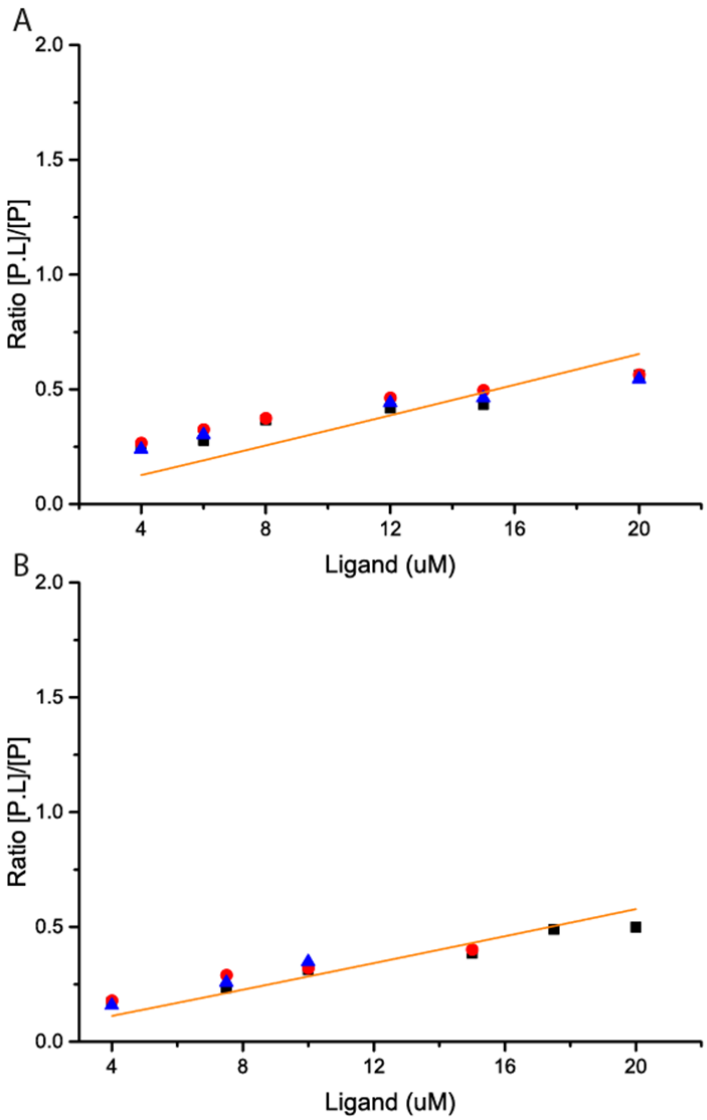

Figure S7. The ratios of the sum of intensities corresponding to bound lopinavir (A), ritonavir (B), and unbound protein are plotted against the respective drug concentrations. The fit was plotted with the equation shown in (C)[2].

(C)

$$\frac{I(\mathrm{PL})}{I(\mathrm{P})} = \frac{1}{2}\left(-1 - \frac{[\mathrm{P}]_0 + [\mathrm{L}]_0}{K_d} + \sqrt{4x\frac{[\mathrm{L}]_0}{K_d} + \left(\frac{[\mathrm{L}]_0 - [\mathrm{P}]_0}{K_d} - 1\right)^2}\right)$$

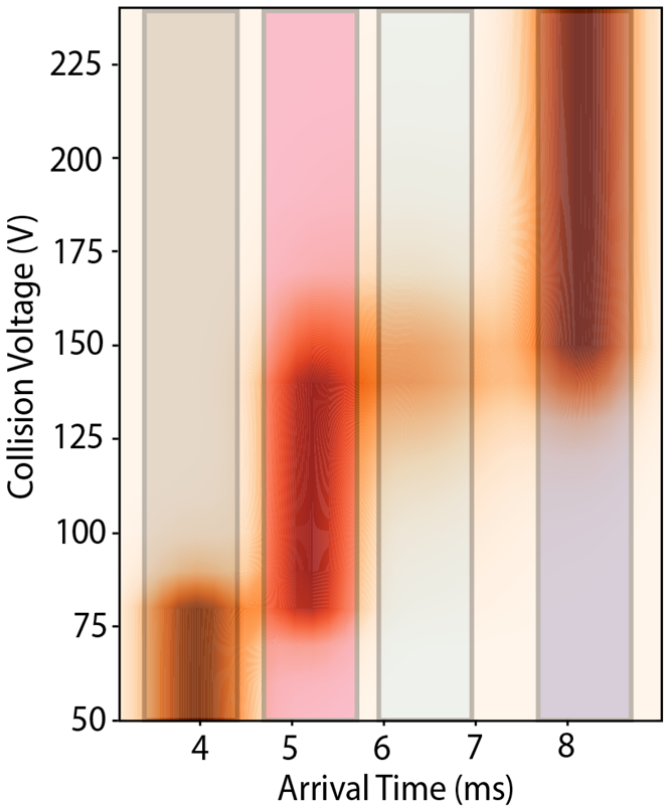

Figure S8. Collision-induced unfolding profile of the 11+ charge state of ZMPSTE24. The ions remain native-like under low activation conditions. A long-lived unfolded state is formed at a collision voltage of 75 V and eventually transitions to a more unfolded form of the protein beyond 140 V.

References:

1 Lee, R. *et al.* Genetic studies on the functional relevance of the protein prenyltransferases in skin keratinocytes. *Hum Mol Genet* **19**, 1603-1617, doi:10.1093/hmg/ddq036 (2010).

2 Erba, E. B. & Zenobi, R. Mass spectrometric studies of dissociation constants of noncovalent complexes. *Annu Rep Prog Chem, Sect C,* **107**, 199-228, doi:10.1039/C1PC90006D (2011).